Department of Aerospace Engineering

Indian Institute of Technology, Bombay

Course Project – AE 651

Design of a Transonic Axial Fan

By

Anubhav Choudhary (180010010)

Atharva Telange (180010014)

TABLE OF CONTENTS

1.Introduction

1.1 Axial compressors

Axial compressors are compressors in which the air flows mainly parallel to the rotational axis. Axial flow compressors have large mass flow capacity, high reliability, and high efficiencies, but have a smaller pressure rise per stage. A typical axial compressor has a series of rotating rotor blades followed by a stationary set of blades called stator that are concentric with the axis of rotation. The compressor blades/vanes are relatively flat in section. Each pair of rotors and stators is referred to as a stage as shown in fig-1. The stator blades are required in order to ensure reasonable efficiency. Without them, the gas would rotate with the rotor blades resulting in a large drop in efficiency. The axial compressor compresses the working fluid by first accelerating the air and then diffusing it to obtain a static pressure increase. The air is accelerated in the rotor and then diffused in the stator. The absolute velocity increases in the rotor and decreases in the diffuser. For successive stages, a saw-teeth pattern for the velocity is obtained, while the static pressure continuously increases in both of the rotor and stator rows of all stages.

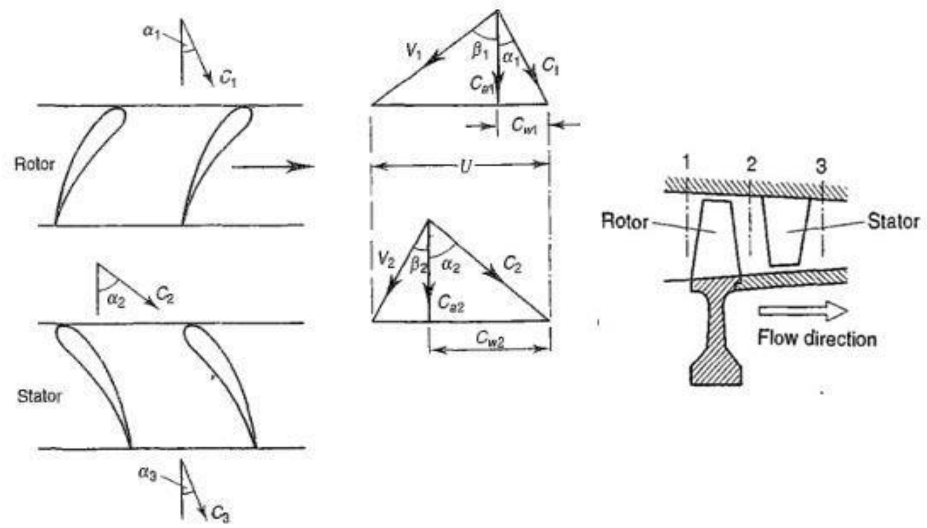

Figure 1-Layout of an axial compressor stage with velocity triangles

Axial compressors are widely used in both aero-engines and industrial gas turbines. Almost all present-day jet engines use axial-flow compressors. The fan in turbofan engines is also an axial compression module which is treated as an axial compressor having a fewer number of blades of very large height, wide chord, and large twist. Based on flow regime in the compressor, it may be classified as subsonic, transonic and supersonic compressors.

1.2 Transonic axial compressors

A transonic compressor is one where the relative flow remains subsonic at inner radii, supersonic at outer radii and transonic region in the middle. Transonic compressors are now successfully used in both aircraft and industrial gas turbines. The fan in turbofan engines is also an axial compression module which is more likely to be a transonic axial fan having a fewer number of blades of very large height, wide chord, and large twist. Early transonic and supersonic compressor designs were failures. The efficiencies were poor and the reliability was not good. It was initially believed that the low efficiencies obtained were due to the shock pattern alone. It was later recognized that the losses were more a result of flow disturbances caused by shocks. Major improvements have been made in blading design, shock optimization, and hub-to-tip design. The present airfoil blade designs are shown in fig-2. The most successful designs are the ones custom designed, based on the controlled diffusion airfoil and shock-free airfoil design concepts. This has enabled high efficiency to be achieved (from 40% in 1940's to nearly 90% currently) with various shock configurations (fig-2).

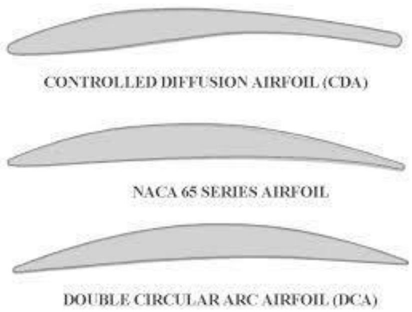

Figure 2-Transonic airfoils for axial compressor

The present trend is towards low aspect ratio and higher Mach number blading, so as to achieve supersonic flow at most radial locations. The number of stages could be reduced for a given pressure ratio, thus enabling substantial savings in weight and size.

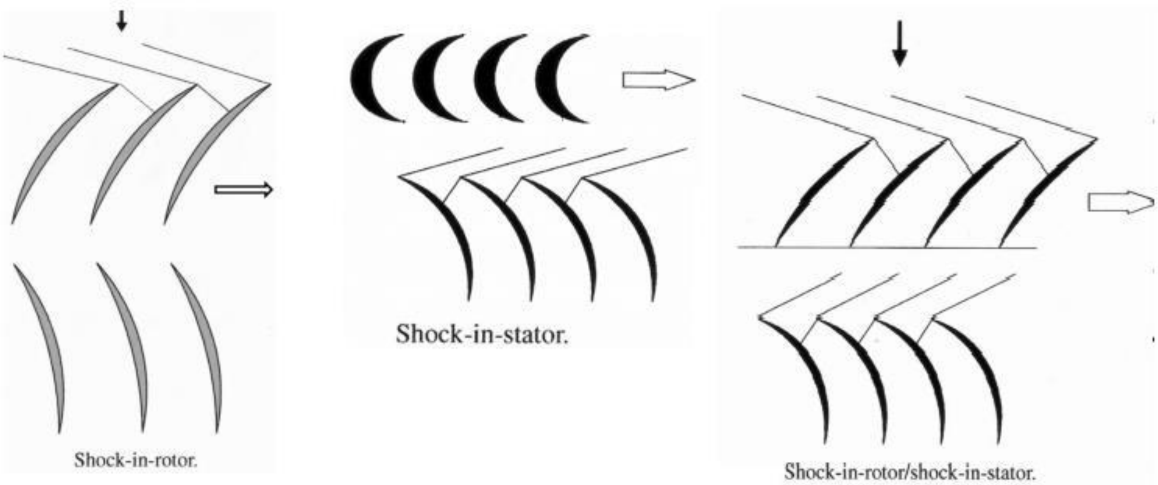

Figure 3-Various shock configurations in transonic compressor

2.Design of Single-Stage Transonic Axial Fan

2.1 Problem statement

Design a single-stage transonic axial fan of following specifications.

Pressure ratio, π_c	**1.6**
Outer diameter (m)	**0.8**
Hub-tip ratio	**0.4**
Rotor speed, N (rpm)	**9500**
Mass flow rate (kg/s)	**24**

2.2 Design Methodology

2.2.1 Setting up the design criteria for transonic stage

- **$(\Delta T_0)_{transonic}$ = 45-55 K**
  The total temperature rise of the transonic stage is to be kept within this limit as per literature as mentioned in [4]. If the rise is being either far beyond this range or much lower than this range, then the stage is more likely to become a supersonic or subsonic stage respectively.

- **$(M1_{rel})_{tip}$ = 1.1-1.7**
  The tip relative Mach number is to be kept within the above range. An increase above the upper threshold leads to unnecessary shock effects, leading to drastic efficiency drop.

- **$(D_h/D_t) \leq 0.4$**
  Since fans tend to handle larger mass flowrates, the hub to tip ratio is usually kept low and it is seen that the given specification itself is meeting this criterion by default.

- **M_a = 0.4-0.7**
  The axial Mach number is to be kept in the above range. Alleviation from this design limit might lead to incidence losses.

2.2.2 Design step-by-step Procedure:

For designing the stage, Multall which is an open-source, CFD based, Turbomachinery design system is used with manually calculated properties (using spreadsheet) been given as input. Following flow-chart summarizes the design methodology in brief.

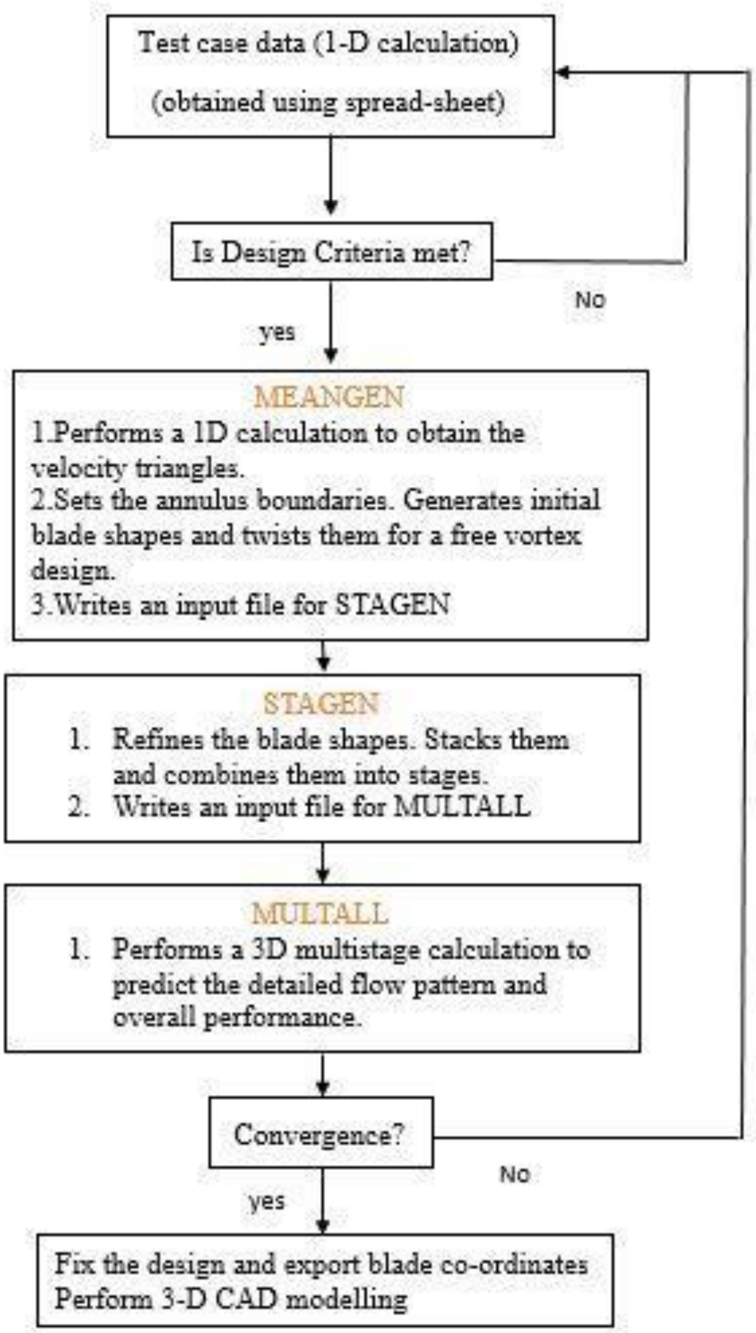

Figure 4-Flow chart describing the step-by-step design approach used

2.2.3 Mean-line Design

Given parameters

Pressure ratio, π_c	1.6
Outer diameter (m)	0.8
Hub-tip ratio	0.4
Rotor speed, N (rpm)	10000 (initially was 9000)
Mass flow rate (kg/s)	24

Assumed Parameter:

Inlet static temperature, T_1(K)	285.15
Inlet absolute Mach number, M_1	0.4
Compressor Efficiency, η_c (%)	90
α_1 (No IGV)	0°

Preliminarily, the design process involved calculation of various flow and blade parameters at the mean-section using empirical relations as follows.

The design is initiated by calculating the parameters at mean section as follows:

1. Inlet absolute velocity (C_1) is calculated from the assumed Mach number:
$$C_1 = M_1 * \sqrt{\gamma R T_1}$$
2. Axial absolute velocity is calculated from the inlet absolute velocity (C_1):
$$C_a = C_1 * \cos(\alpha_1)$$
3. Blade speed at mean diameter:
$$U_{mean} = \frac{\pi D_{mean} N}{60}$$
4. Work done on the fan/Compressor is calculated based on the pressure ratio and assumed efficiency:
$$\Delta h_0 = \frac{C_p T_{01}}{\eta_f}\left(\pi_c^{\frac{\gamma-1}{\gamma}} - 1\right)$$
5. Now, by equating thermodynamic work and aerodynamic work:
$$\Delta h_0 = U_{mean}\, C_a * (\tan(\alpha_2) - \tan(\alpha_1))$$
$$\alpha_2 = \tan^{-1}\left(tan(\alpha_1) + \frac{\Delta h_0}{U_{mean} c_a}\right)$$
6. Using the axial flow velocity and peripheral velocity, flow coefficient is calculated:
$$\Phi = \frac{C_a}{U_{mean}}$$
7. Blade angles at inlet and exit can be calculated by:
$$\frac{1}{\phi} = \frac{U_{mean}}{C_a} = \tan(\beta_1) + \tan(\alpha_1) = \tan(\beta_2) + \tan(\alpha_2)$$
$$\beta_1 = \tan^{-1}\left(\frac{1}{\phi} - tan(\alpha_1)\right)$$
$$\beta_2 = \tan^{-1}\left(\frac{1}{\phi} - tan(\alpha_2)\right)$$
8. Stage loading is calculated from stage enthalpy change and peripheral velocity:
$$\psi = \frac{\Delta h_0}{U_{mean}^2}$$

9. Degree of reaction is calculated from:

$$R_x = 1 - \frac{\phi}{2}(\tan(\alpha_2) + \tan(\beta_2))$$

From the above given parameters and using the values in the formulae, we calculate as shown below:

From inlet absolute Mach number, $M_1 = 0.4$,

$$C_1 = C_a = 135.430 \text{ m/s}$$

- Mean peripheral Velocity (U_{mean}):

$$U_{mean} = \frac{\pi * 0.56 * 10000}{60} = 293.215 \text{ m/s}$$

- Work done/ Stage enthalpy change from pressure ratio:

$$\Delta h_0 = \frac{C_p T_{01}}{\eta_f}\left(\pi_c^{\frac{\gamma-1}{\gamma}} - 1\right) = \frac{1004.85 * 294.278}{0.9}\left(1.6^{\frac{1.4-1}{1.4}} - 1\right) = 47220.570 \frac{KJ}{kg}$$

- Flow angle from stage enthalpy:

$$\alpha_2 = \tan^{-1}\left(tan(\alpha_1) + \frac{\Delta h_0}{U_{mean} c_a}\right) = \tan^{-1}\left(tan(0) + \frac{47220.570}{293.215 * 135.430}\right) = 49.937°$$

- Flow Coefficient:

$$\Phi = \frac{C_a}{U_{mean}} = \frac{135.430}{293.215} = 0.46187$$

- Blade Angles at inlet & exit of rotor:

$$\beta_1 = \tan^{-1}\left(\frac{1}{\phi} - tan(\alpha_1)\right) = 65.208°$$

$$\beta_2 = \tan^{-1}\left(\frac{1}{\phi} - tan(\alpha_2)\right) = 44.302°$$

- Stage Loading:

$$\psi = \frac{\Delta h_0}{U_{mean}^2} = 0.549$$

- Degree of Reaction:

$$R_x = 1 - \frac{\phi}{2}(\tan(\alpha_2) + \tan(\beta_2)) = 0.725$$

3. 3-D Design: Using Free Vortex Law

Free vortex method is one of the simplest design methods in axial compressors. It is based on the general radial equilibrium equation with the following simplifications.

1. Assuming *constant specific work* at all radii, $\frac{dh_0}{dr} = 0$

$$\therefore C_a \frac{dC_a}{dr} + C_u \frac{dC_u}{dr} + \frac{C_u^2}{r} = 0$$

2. Assuming *constant axial velocity* at all radii, $\frac{dC_a}{dr} = 0$

$$\therefore \ C_u \frac{dC_u}{dr} + \frac{C_u^2}{r} = 0$$

$$\frac{dC_u}{C_u} = -\frac{dr}{r}$$

Figure 5- Free vortex law assumptions

Integrating, we get

$$\boldsymbol{r.c_u = constant}$$

Thus, the whirl velocity component of the flow varies inversely with radius, which is known as free vortex. Thus, the following three variables (h_0, C_a, r. C_u) are not varying in the radial direction. Keeping these implications, free vortex law is used to calculate flow properties along the annulus at the rotor inlet and outlet as shown below.

- The tangential absolute velocity along the annulus is calculated using,

$$\mathbf{r.c_u = r_m.c_m}$$

- The absolute flow angles at rotor inlet and outlet along annulus are calculated by,

$$\mathbf{r.\tan(\alpha_1)_r = r.\tan(\alpha_1)_m}$$

- The relative flow angles at rotor inlet and outlet along annulus are calculated from,

$$\mathbf{\tan(\alpha_1)_r + \tan(\beta_1)_r} = \boldsymbol{U_r/(C_a)_r}, \text{ where } U_r = U_m.\ (D/D_m)$$

The results obtained in the spread-sheet are compared with the 'Stagen' results and by comparison, both are found to be matching each other. Various data were tabulated and plotted to check the feasibility of design and to have a clear-cut view of variation of various aerodynamic parameters as shown below.

	Hub						Mean						Tip
r(m)	0.16	0.18	0.2	0.22	0.24	0.26	0.28	0.3	0.32	0.34	0.36	0.38	0.4
cw_1(m/s)	0	0	0	0	0	0	0	0	0	0	0	0	0
cw_2(m/s)	281.8270225	250.5129089	225.461618	204.9651073	187.8846817	173.4320139	161.0440129	150.3077453	140.9135113	132.6244812	125.2564545	118.6640095	112.730809
R(r/rm)	0.5714285714	0.6428571429	0.7142857143	0.7857142857	0.8571428571	0.9285714286	1	1.071428571	1.142857143	1.214285714	1.285714286	1.357142857	1.428571429
U_1(m/s)	167.5516082	188.4955592	209.4395102	230.3834613	251.3274123	272.2713633	293.2153143	314.1592654	335.1032164	356.0471674	376.9911184	397.9350695	418.8790205
U_2(m/s)	167.5516082	188.4955592	209.4395102	230.3834613	251.3274123	272.2713633	293.2153143	314.1592654	335.1032164	356.0471674	376.9911184	397.9350695	418.8790205
Rx	0.1589844301	0.3354938707	0.4617500352	0.5551653184	0.6262153022	0.6815088966	0.725382671	0.7607777934	0.7897461075	0.8137543375	0.8338734677	0.8509002868	0.8654375088
ca_1(m/s)	135.4300714	135.4300714	135.4300714	135.4300714	135.4300714	135.4300714	135.4300714	135.4300714	135.4300714	135.4300714	135.4300714	135.4300714	135.4300714
ca_2(m/s)	135.4300714	135.4300714	135.4300714	135.4300714	135.4300714	135.4300714	135.4300714	135.4300714	135.4300714	135.4300714	135.4300714	135.4300714	135.4300714
ΔT0(K)	46.99265647	46.99265647	46.99265647	46.99265647	46.99265647	46.99265647	46.99265647	46.99265647	46.99265647	46.99265647	46.99265647	46.99265647	46.99265647
UΔcw(J/kg)	47220.57085	47220.57085	47220.57085	47220.57085	47220.57085	47220.57085	47220.57085	47220.57085	47220.57085	47220.57085	47220.57085	47220.57085	47220.57085
α1(deg)	0	0	0	0	0	0	0	0	0	0	0	0	0
α2(deg)	64.33370245	61.60384989	59.00764401	56.5453874	54.21537627	52.0143358	49.93781988	47.98056052	46.13676147	44.40033621	42.76509487	41.22488616	39.77370146
β1(deg)	51.05178258	54.30355395	57.11204041	59.55101499	61.68158708	63.55386073	65.20876438	66.67973931	67.994182	69.17462908	70.23971118	71.20491311	72.08317691
β2(deg)	-40.15755443	-24.60441439	-6.747038764	10.62996047	25.10091918	36.12265346	44.30230352	50.42485776	55.10765022	58.77739942	61.72030944	64.12933754	66.13695063
β1-β2 (deg)	91.20933701	78.90796834	63.85907917	48.92105453	36.58066789	27.43120727	20.90646085	16.25488154	12.88653178	10.39722966	8.519401744	7.075575566	5.946226282
Vrel_1	215.4410491	232.1031669	249.4117333	267.241171	285.4939096	304.0937348	322.980688	342.1072175	361.4352914	380.9342327	400.5790903	420.3494067	440.2282795
Vrel_2	177.200944	148.9545431	136.3745291	137.7947639	149.5536168	167.6619254	189.2367754	212.5761625	236.7508095	261.2642359	285.8524887	310.3765925	334.7656369
Vw_1	167.5516082	188.4955592	209.4395102	230.3834613	251.3274123	272.2713633	293.2153143	314.1592654	335.1032164	356.0471674	376.9911184	397.9350695	418.8790205
Vw_2	-114.2754143	-62.01734969	-16.02210777	25.41835398	63.44273061	98.83934946	132.1713015	163.85152	194.1897051	223.4226862	251.734664	279.27106	306.1482115
C_1	135.4300714	135.4300714	135.4300714	135.4300714	135.4300714	135.4300714	135.4300714	135.4300714	135.4300714	135.4300714	135.4300714	135.4300714	135.4300714
C_2	312.6783889	284.777144	263.0099721	245.6664394	231.6073355	220.0453764	210.4197669	202.3208406	195.4428865	189.5535736	184.473531	180.0623542	176.2087953
StageLoading	1.68203114	1.329012259	1.07649993	0.8896693632	0.7475693955	0.6369822068	0.5492346579	0.4784444131	0.420507785	0.3724913251	0.3322530647	0.2981994265	0.2691249824
Flow_Coefficient	0.808288699	0.7184788436	0.6466309592	0.5878463266	0.5388591327	0.4974084302	0.4618792566	0.4310873061	0.4041443495	0.3803711525	0.3592394218	0.3403320838	0.3233154796
Mrel_1	0.6363721327	0.6855888788	0.7367151119	0.7893799004	0.8432950398	0.8982354073	0.9540238968	1.010520049	1.067611526	1.125207713	1.183234908	1.241632686	1.300351118

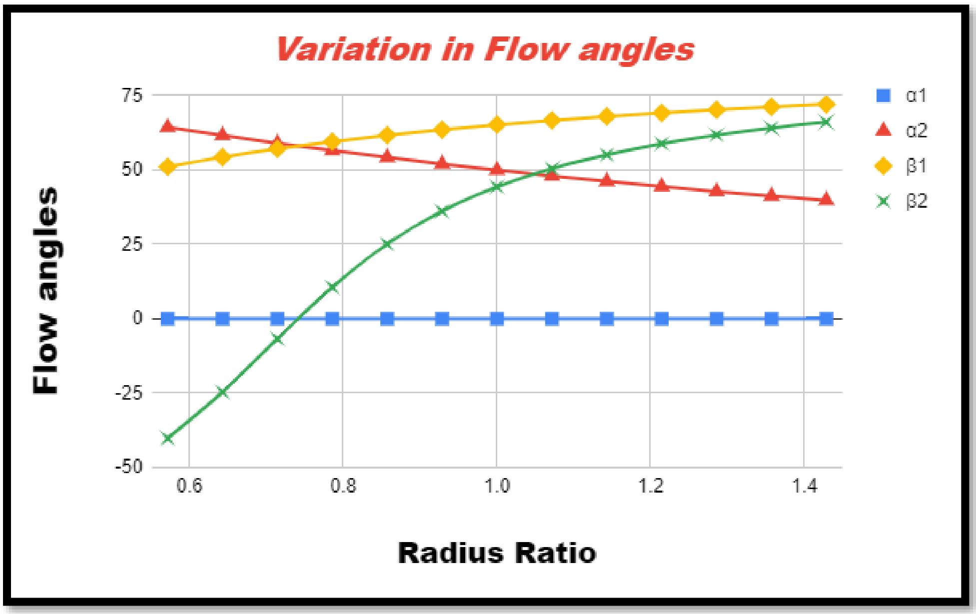

The above plot shows the increase of blade angles as we move towards the tip but the difference is small (Table-(1)), whereas at the hub, the difference is too large indicating large flow turning (β1-β2) occurring at the hub as it is used to be.

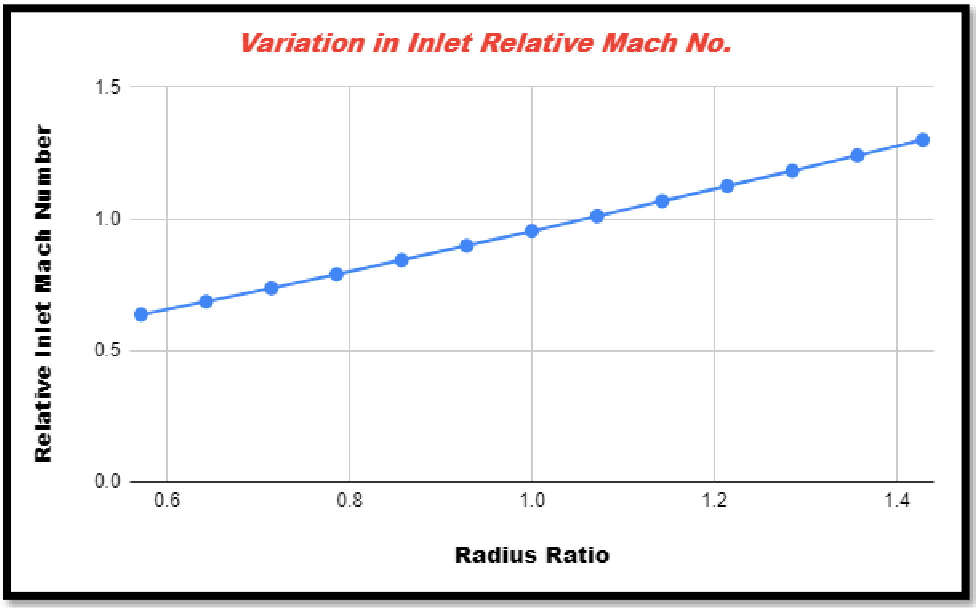

Variation of inlet rotor relative Mach number along annulus shows its increase along annulus. It is also to be noted that the Mmax occurs at the tip with a value of 1.44 which is tend to lie within the reasonable range for transonic stage satisfying the design criteria discussed earlier. Also, it observed for a transonic stage to happen, there must be a subsonic regime at the hub, a sonic radius in middle and supersonic regime at the tip as mentioned in the figure below.

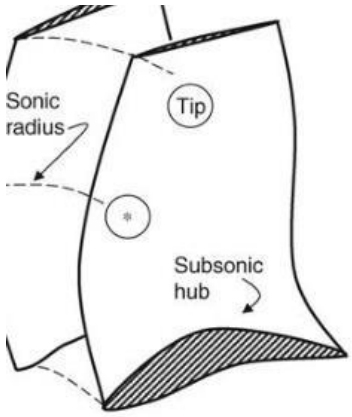

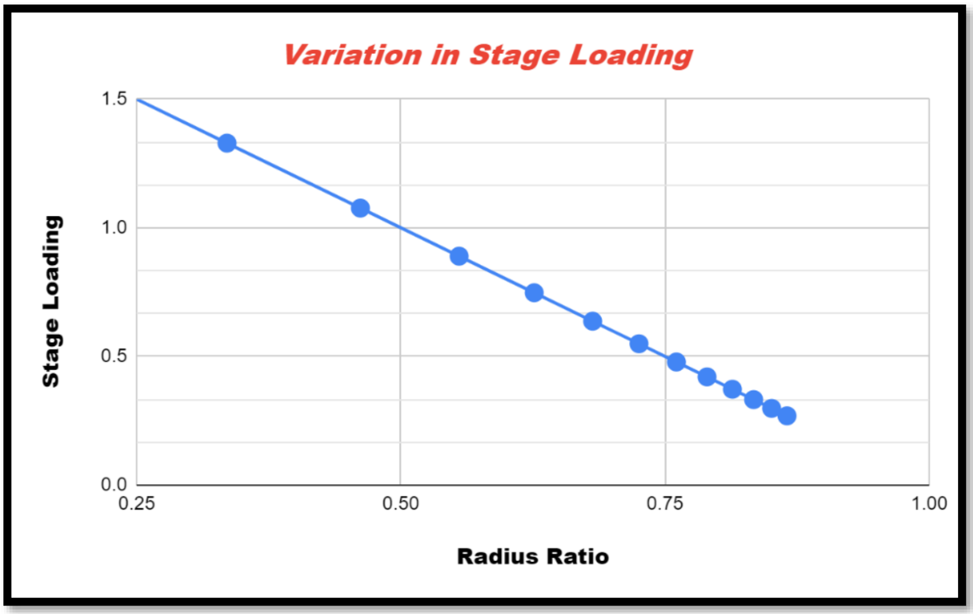

The stage loading at the hub is found to be higher as it is used to be indicated by the plot.

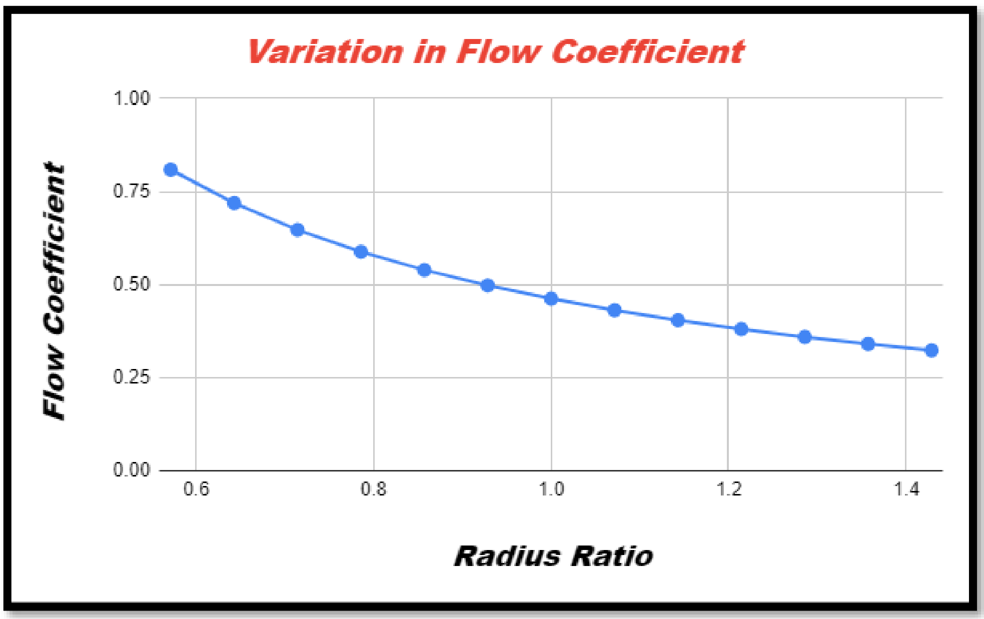

By assumption of constant axial velocity and also constant axial velocity ($dca\ dr$ = 0) along annulus by free vortex law, the flow co-efficient is found to decrease along annulus due to increase in blade speed

4. Blade Geometry:

The blade sections can be generated in a variety of ways in Multall:

1. A pre-existing blade shape may be input by reading in its co-ordinates
2. The blade shape is input as a table of camber line angle and blade thickness against fraction of meridional chord.

The blade profiles are generated on a plane (x, y) surface but are then transformed into the (m, ϴ) co-ordinate system of the stream-wise surfaces such that the x-value becomes the meridional distance m and the y value defines the value of ϴ on the stream-wise surface using

$$\theta - \theta_1 = \int_{r_1}^{r} dy \Big/ r$$

This ensures that a flat plate on the (x,y) surface transforms into a log spiral on the (m, θ) surface.

The following blade co-ordinates were generated in Multall and modelling is done using tools like —

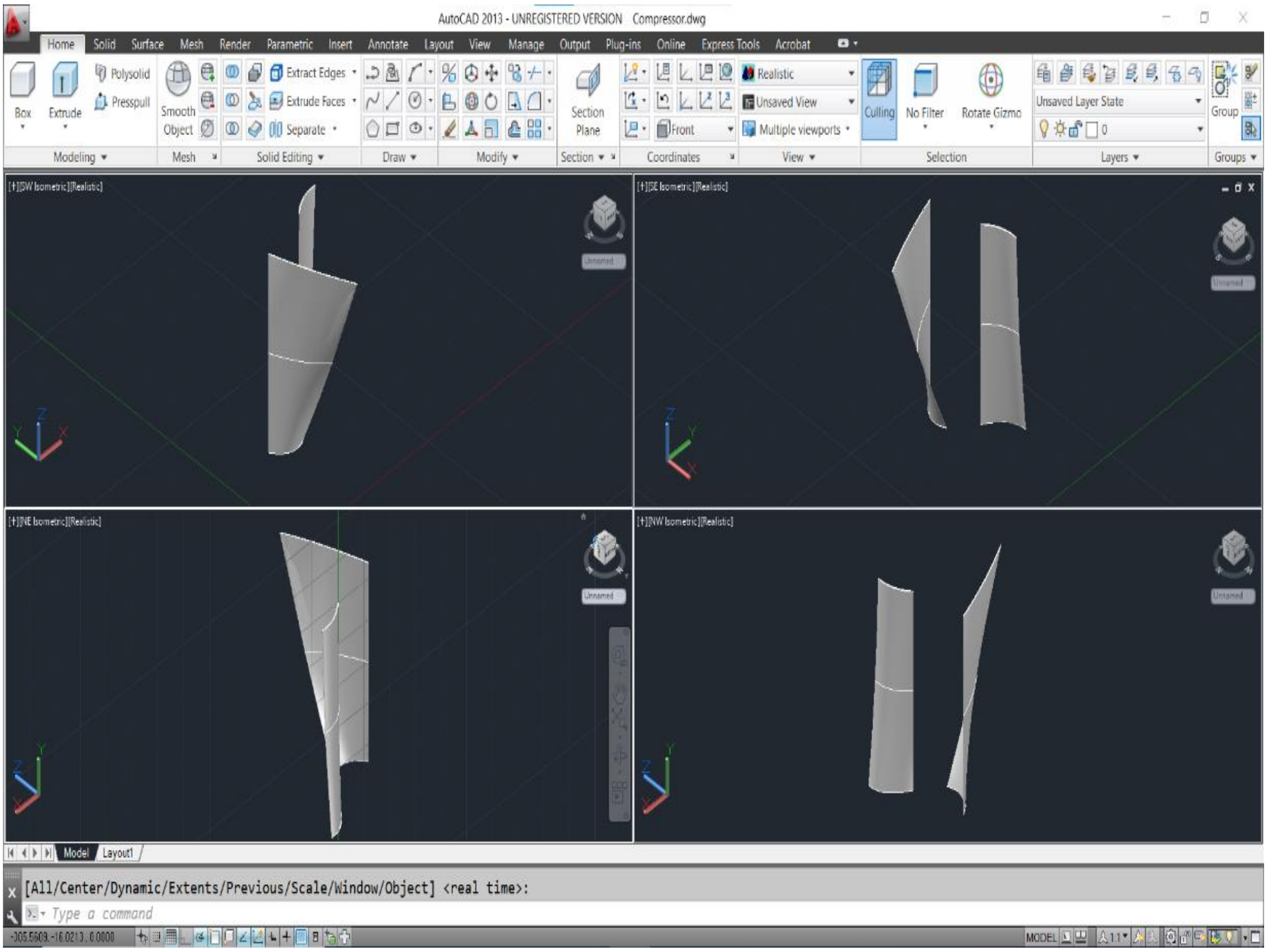

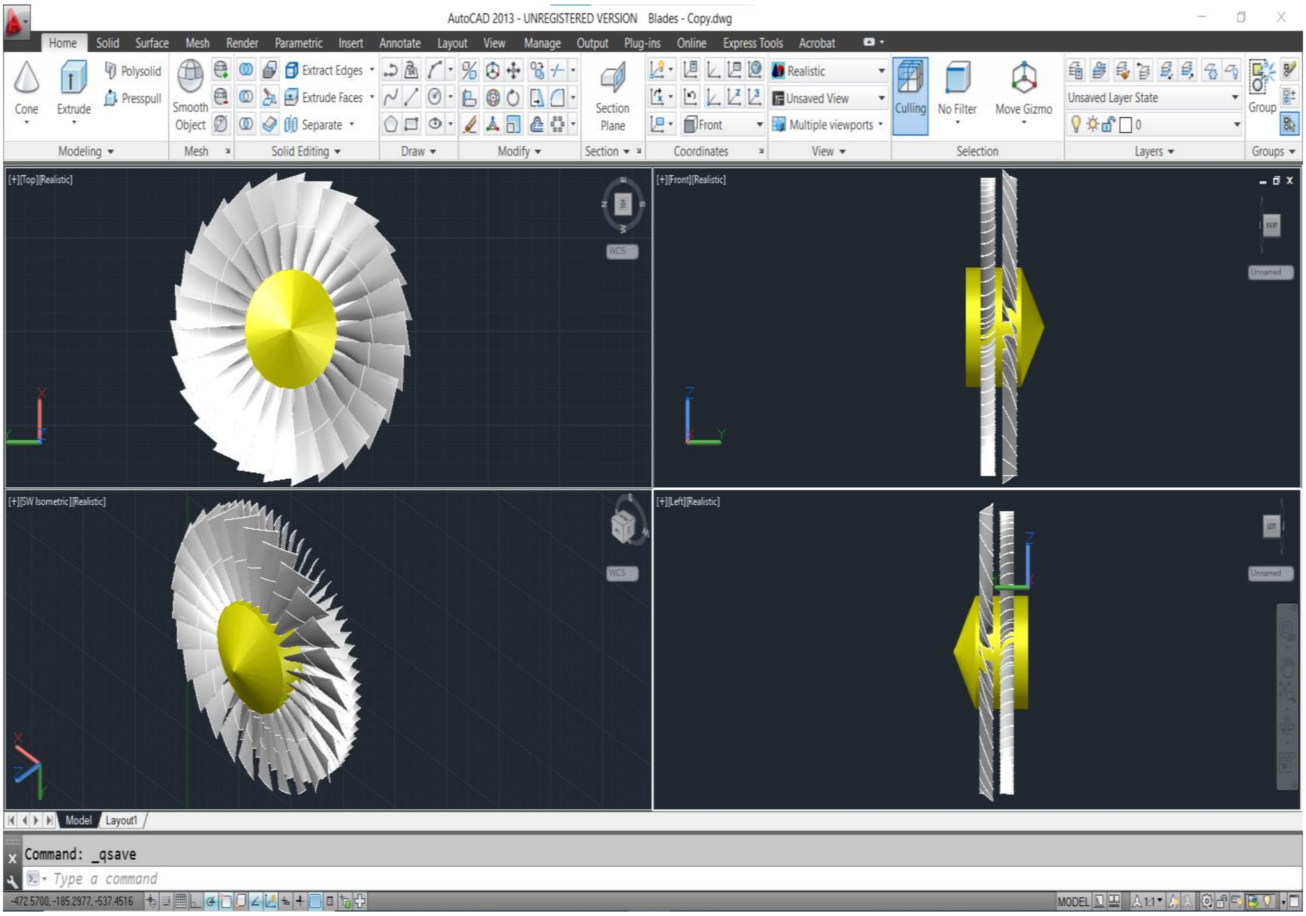

5. Conclusion

- Manual and computational analysis have been carried out for design of transonic stage axial fan low hub-to-tip ratio (0.4) with a rotor rotational speed of 10000 rpm.
- Certain reasonable assumptions were made during the design process and a check has been made whether such assumptions could satisfy the primitive design criteria.
- Manually, calculated 1-D design values were compared with the obtained 'meangen' values for given specifications and the design process is carried further.
- 3-D design analysis were carried using 'Free Vortex Law' and similarity comparison has been made with the 'Stagen' values.
- The output from 'Stagen' file has been given as input to 'Multall' file to carry out the simulation and convergence is checked (Inflow = Outflow)
- Once the convergence is met, blade geometry is finalized after appropriate optimization and 3-D CAD models were generated.

References

1. H. Cohen, HIH Saravanamuttoo, GFC Rogers, Gas Turbine Theory, Fifth Edition, Pearson Education Ltd.
2. Ahmed F. El-Sayed, Fundamentals of Aircraft and Rocket Propulsion, Springer Edition.
3. Class lecture slides, "Aerodynamics of Compressors and Turbines" by Prof. A.M. Pradeep
4. Sample Reports given for the course AE-651

Appendix

Blade Geometry Co-ordinates for finalized design and input file for meangen

The blade geometry for finalized design extracted from Multall is included in the following link:

Blade Geometry Co-ordinates

Input file for meangen